Journal of Macromolecular Science, Part A
Publication details, including instructions for authors and subscription information:
http://www.informaworld.com/smpp/title~content=t713597274

A Facile Approach to Design Plaster of Paris Based Polymer Nanocomposites for Possible Use as Bone Implants

Seeta Shukla[a]; A. K. Bajpai[a]
[a] Bose Memorial Research Laboratory, Government Autonomous Science College, Jabalpur, M.P, India

Online publication date: 05 July 2010

To cite this Article Shukla, Seeta and Bajpai, A. K.(2010) 'A Facile Approach to Design Plaster of Paris Based Polymer Nanocomposites for Possible Use as Bone Implants', Journal of Macromolecular Science, Part A, 47: 8, 849 — 860
To link to this Article: DOI: 10.1080/10601325.2010.492269
URL: http://dx.doi.org/10.1080/10601325.2010.492269

Journal of Macromolecular Science, Part A: Pure and Applied Chemistry (2010) **47**, 849–860

ISSN: 1060-1325 print / 1520-5738 online
DOI: 10.1080/10601325.2010.492269

A Facile Approach to Design Plaster of Paris Based Polymer Nanocomposites for Possible Use as Bone Implants

SEETA SHUKLA and A. K. BAJPAI*

Bose Memorial Research Laboratory, Government Autonomous Science College, Jabalpur (M.P), India

Received January 2010, Accepted March 2010

The controlled integration of organic and inorganic components confers natural bone with superior mechanical properties. The external use of calcium sulphate in the form of Plaster of Paris (PP) has been well established but its possible use inside the human body as bone void filler is only a recent phenomenon. Since PP serves as potential material in various biomedical applications an attempt has been made in the present study to design and fabricate biomimetic bone-like composite materials by polymerizing 2-hydroxyethyl methacrylate (HEMA) with a redox system in the immediate presence of PVA and PP taken in different weight ratios. The prepared composite materials were characterized by various techniques like Fourier transform infrared spectroscopy (FTIR), X-ray diffraction (XRD) analysis, scanning electron microscopy (SEM). *In vitro* tests were carried out, to study the water-uptake and dissolution profiles of the composites and this was done by observing the swelling behavior of the material in distilled water and phosphate buffer saline (PBS) till equilibrium swelling was achieved. Furthermore, *in vitro* blood compatibility of prepared materials was also evaluated using protein adsorption, percentage haemolysis, blood clot formation and platelet adhesion tests. The morphology of composite studied by scanning electron microscopy (SEM) suggested the size of the aggregated crystals varies in the range 10 to 20 μm having an average width of 5 μm. The composites showed satisfactory mechanical properties as is evident from the varying compressive strength and modulus in the range 4.5 to 16 MPa and 33 to 200 MPa, respectively. The water sorption behavior was found to be dependent on the chemical composition of the matrix. The porosity of composite varied between 28 to 52%. The *in vitro* blood compatibility indicated that the adsorption of bovine serum albumin (BSA) varied from 0.020 to 0.033 $mg \cdot g^{-1}$, the percentage haemolysis was between 8.2 to 23.0% and the weight of blood clot formed on the composite surfaces were found in the range 9 to 33 mg.

Keywords: Nanocomposite, characterization, biocompatibility, swelling ratio

1 Introduction

Bone related injuries causing hospitalization due to fractures and grafting procedures have become a global phenomenon (1, 2). Osteoporosis is a disease of bone-loading to an increased risk of fracture, during which bone mineral density is reduced, micro architecture is disrupted and the amount and variety of non-collagenous proteins in bone are altered (3). The continued increase in the age of population has generated higher demands for bone grafting (4). To address the need for intervention in these causes, many materials are currently in use to repair or replace bone that has been damaged due to trauma or disease such as large bone tumors, defects, and fractures. These include natural autografts and allografts, as well as a variety of biomaterials based on ceramics, metals, polymers and a host of composites comprising polymer matrix and bioactive ceramic, fillers etc. All these materials have been successfully used in substitution of bone tissue and in many other orthopedic applications (5). Ideally, a scaffold which is going to be implanted should have the following characteristics such as: (a) Three dimensional and highly porous with an interconnected pore network for all growth and nutrients and metabolic waste; (b) Biocompatible and bioresorbable with a controllable degradation and resorption rate; (c) Suitable surface chemistry for all attachment proliferations, and (d) Mechanical properties to match those of the tissues of the site of implantation (6).

Bioabsorbable non-allogenic bone substitutes (ceramics) mainly composed of hydroxyapatite, like tricalcium phosphate or calcium sulphate is now commercially available for clinical use (7, 8). Attempts have been made to form high strength consolidated hydroxyapatite ceramics using natural and synthetic polymers (9). Hydroxyapatite is a good biocompatible material, and when used or impregnated with HEMA and PVA based hydrogels, it

*Address correspondence to: A. K. Bajpai, Bose Memorial Research Laboratory, Government Autonomous Science College, Jabalpur (M.P), India. Fax: 0761-2625514; E-mail: akbmrl@yahoo.co.in; akbajpailab@yahoo.co.in

shows enhanced mechanical properties (10). Grafting of hydroxyethyl methacrylate (HEMA) to the surface of the reactive co-precipitate has resulted in bonding between the monomer and co-precipitate. The mineral nucleating potential of hydroxyl ligands identified here broadens the design parameters for synthetic bone like composites and suggests a potential role for hydroxylated protein in bone mineralization (11). A material to be used in such applications must exhibit adequate mechanical properties coupled with controlled degradation rates and appropriate biological behavior in terms of interaction with living tissues (12).

Recent research has been directed toward the wetting ability of HEMA which increases the infusion and impregnation of resin monomers into the demineralized dentinal matrix. Thus, the interfacial hybrid zone formed by HEMA must have played an important role in enhancing the bonding of resin composite. Other research groups have also suggested the importance of hydrogen bond formation involved in the dentine bonding mechanism (13). The availability and suitability of traditional autogenous or homogenous prosthetic elements are severely limited and as a result immense interest has been focused on the use of synthetic materials that are found to be biocompatible after promising opportunities for both implantable biomedical devices and in the lives of patients. However, mechanical testing must be performed to determine how exactly these biocompatible materials can be used as substitute for diseased or damaged tissue. Mechanical testing is common methodology to evaluate the performance of implant materials.

Although the nanoscale modeling of synthetically manufactured hybrids and composites is still in infancy, mimicking natural microstructures, while using synthetic molecules, may lead to new generation materials whose toughness characteristics will be comparable with the materials available in the nature. A formidable challenge remains on the optimizations of their morphology and bioactivity in these novel hybrid composites (14). Existing orthopedic implants typically consist of single bioinert materials such as metals, ceramics or polymers and offer relatively cores combination of two or three components (15). The development of bone-like composites with improved mechanical properties and enhanced biocompatibility calls for a biomimetic approach using natural bone as guide (16). In the present work, PHEMA based hydrogels have been chosen for this purpose due to their well established biomedical properties and ease of functionalization (17). PHEMA is particularly attractive for biomedical engineering application because its physical properties can be easily manipulated through formulation chemistry and it has been extensively used in biomedical applications (18). Although polymers of HEMA are hydrophilic and biocompatible, however, often put limitations particularly in those applications where the matrix has to bear stress. Thus, polyvinyl alcohol (PVA), a synthetic polymer of known recognition in biomedical community, has been employed as a supporting matrix to strengthen the resulting PHEMA network. Plaster of Paris is the hemihydrates of $CaSO_4$-$2H_2O$ and is manufactured by heating gypsum ($CaSO_4 \cdot 2H_2O$) in such a way that it loses three quarters of its water of crystallization:

$$CaSO_4 \cdot 2H_2O \longrightarrow CaSO_4 \cdot {}^1/_2H_2O + 1{}^1/_2H_2O$$

Once hemihydrates of $CaSO_4$ is mixed with water, it solidifies:

$$CaSO_4 \cdot {}^1/_2H_2O + 1{}^1/_2H_2O \longrightarrow CaSO_4 \cdot 2H_2O$$

The mineral components taken in the present work is PP which has quite inexpensive, easily sterilizable and completely resorbable. Moreover, its use in fabricating biomaterial is largely reported in the literature (19).

2 Experimental

2.1 Materials

Plaster of paris (Medical grade) was supplied by E. Merck and used as received. Polyvinyl alcohol (mol. wt 14000, 98% hydrolyzed) was purchased from E. Merck, India and used without any pretreatment. 2-Hydroxyethyl methacrylate (HEMA) and ethylene glycol dimethacrylate (EGDMA) were used as monomer and crosslinking agent, respectively. Potassium persulphate (KPS) and potassium metabisulphite (MBS) obtained from Loba Chemicals India, were employed as polymerization activator and initiator, respectively. All chemicals were of analytical grade and doubly distilled water was used throughout the experiments.

2.2 Methodology

2.2.1. *Purification of Monomer*

Due to poor stability of HEMA, high purity of the monomer is essentially required in hydrogels synthesis as the presence of impurities may greatly affect the swelling characteristics of the end polymer. Degradation of monomer during transportation and storage at ambient temperatures may result in increased levels of methacrylic acid (MAA) and the natural occurring crosslinker EGDMA. As illustrated in Figure 1, the HEMA monomer readily undergoes three common reactions:

(1) HEMA may hydrolyze at the ester linkage to form MAA and ethylene glycol;
(2) two molecules of HEMA may transesterify to form the cross linker and ethylene glycol;
(3) monomer may polymerize at the double bond resulting in oligomer and polymer.

Although an inhibitor such as hydroquinone (300 ppm) is normally added to minimize the later reactions, an ultra purity is desired for reliable experimental data.

The impurity of MAA in HEMA monomer was removed by stirring the monomer with 15% by weight of anhydrous

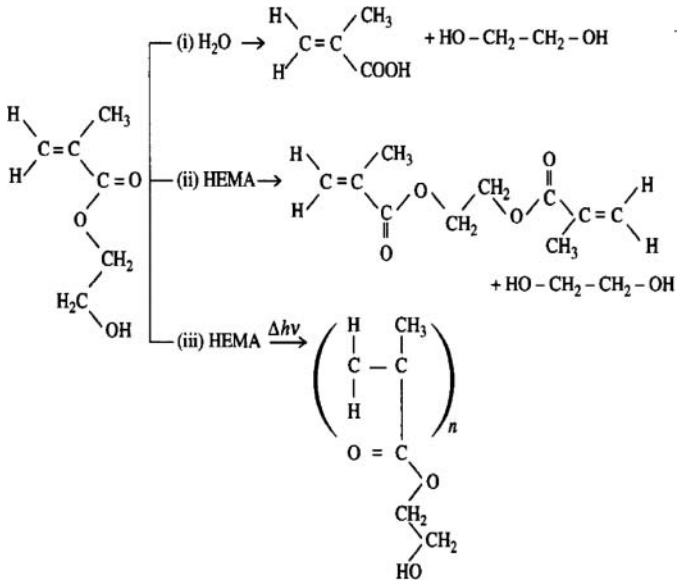

Fig. 1. Synthesis of monomer HEMA.

sodium carbonate for 3 h at 24°C, then vacuum filtering through Whatman filter papers. The yield on an initial volume of 100 mL of HEMA was 89%.

The impurity of EGDMA was then removed by first dissolving the above treated monomer in three times its volume of distilled water. Four extractions were performed with 50 mL of 1:1 (volume) mixture of carbon-tetrachloride and cyclohexane, allowing the layers to separate for 30 min between two extractions. The organic layer containing EGDMA was discarded after each extraction and the aqueous phase was placed under vacuum to remove any remaining organic solvent. The HEMA was then salted out with 100 g of NaCl, then dried with anhydrous sodium sulphate, and filtered.

The partially purified HEMA monomer was vacuum distilled in the presence of 1 g of hydroquinone (added to prevent polymerization) at 60 mm Hg and after distillation; the pure HEMA was transferred to an opaque glass bottle and stored at 4°C until use.

2.2.2. *Purity of HEMA*

The purity of distilled HEMA was determined by high-pressure liquid chromatography (HPLC), [Backmen System (Gold 127)] equipped with a ultraviolet detector, a 25 cm ×46 mm id separation columns ODS (C_{18}), 5 μm particle size. The UV detector was set at 217 nm. The mobile phase was methanol-water (60:40 v/v) and the flow-rate was kept at 1 mL/min. All samples were diluted with pure methanol to 1/1600. 10 μL samples were injected for each analysis. Samples of known concentrations of MAA and EGDMA were injected into the HPLC and the resultant chromatogram was used to construct a standard curve of known concentrations vs. area under the curve. The chromatograph showed two distinct peaks (chromatogram not shown). The first peak, at 3.614 min was identified as MAA. The next peak at 5.503 min was the major peak due to HEMA monomer. The amounts of impurities of MAA and EGDMA in the monomer samples were found to be less than 0.01 mol% MAA and 0.001 mol% EGDMA

2.2.3. *Preparation of PP-HEMA Nanocomposite*

In order to achieve the desired polymer matrix, a free radical initiated polymerization method described elsewhere was adopted (20). In brief, 10 mL PVA solution (10% w/v) was taken with 16.4 mM purified HEMA (2 hydroxyethyl methacrylate) monomer in a Petridish. Then, ethylene glycol (71.6 mM) as a co-solvent, EGDMA (1.06 mM) as a crosslinker, and PP (4.0 g) were added to this mixture. To initiate the polymerization reaction, a redox couple comprising of 1 mL each of degassed solutions of potassium persulphate (10 mg/10 mL) and potassium metabisulphite (90 mg/10 mL) were added to the reaction mixture and polymerization was allowed to proceed for 24 h at room temperature, to obtain a slab of the hydrogel. The preparation of nanocomposite may be schematically shown in Figure 2.

2.3 Characterization

2.3.1. *FTIR Studies*

IR studies of the powdered specimens were recorded on a Perkin-Elmer (1000 Paragon, Shimadzu) spectrophotometer. Prior to analysis, KBr pellets were prepared by mixing

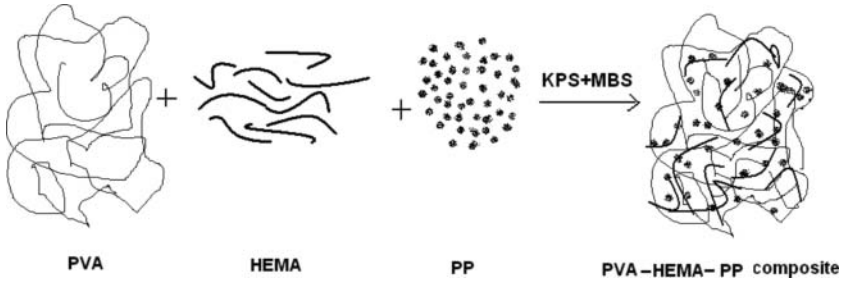

Fig. 2. Schematic diagram for the preparation of PP-HEMA nanocomposite.

1:10 of sample: KBr (wt/wt) followed by uniaxillary pressing the powders under vacuum. The spectra were obtained between 4400 cm^{-1} −450 cm^{-1} at 2 cm^{-1} resolution.

2.3.2. *XRD Studies*

The XRD apparatus Philips PW1820 powder diffractometer, was used to investigate the crystallinity and phase content of PP-HEMA composites. The diffraction data were collected from 2° to 60°, 2θ values with a step size of 0.02° and counting time of 2 s $step^{-1}$ at λ i.e., 1.54 A°.

2.3.3. *Scanning Electron Microscopy*

For studying the morphology of the prepared composites SEM was carried out on STEREO SCAN, 430, Lecica SEM, USA.

2.3.4. *Water Sorption Measurements*

The extent of swelling was determined by a conventional gravimetric procedure as reported in the literature (21). In a typical experiment, pre-weighed pieces of PP-HEMA composites were allowed to swell in distilled water for a pre-determined time period (up to equilibrium swelling). Thereafter, the pieces were taken out from the water and gently pressed in- between the two filter papers to remove excess of water and finally weighed. The swelling ratio was calculated by the Equation 1:

$$\text{Swelling Ratio} = \frac{\text{Weight of Swollen gel}}{\text{Weight of dry gel}} \qquad (1)$$

2.3.5. *Porosity Determination*

The apparent porosity of a porous scaffold can influence its mechanical strength, permeability, and presence of structural defects (22). In the present work, the porosity was determined by the method reported in literature (23) In brief, the known volume and weight of the samples noted as Vo and Wo, respectively were immersed into the dehydrated alcohol for 48 h until absorbing dehydrated alcohol saturated the samples. The weight gained by the sample is measured as W_1. Finally the porosity (P) of the open pores in the composites were evaluated using formula given in Equation 2:

$$P = \frac{W_1 - W_0}{PV_0} \qquad (2)$$

Where p is the density of the dehydrated alcohol

2.3.6. *Blood Compatibility*

Materials to be used in medical applications must meet certain criteria and regularity requirements. The surface of biomaterials is believed to play an important role in determining biocompatibility of materials that come into contact with flowing blood. The formation of a clot is the most undesirable but frequently occurring event that restricts the clinical acceptance of a material to be used as a biomaterial. Therefore, certain test procedures have been developed and they need to be employed to judge the haemo-friendly nature of the materials.

2.3.6.1. *Protein (BSA) adsorption.* The foremost event occurring at the interface of the blood material contact is the adsorption of plasma proteins (bovine serum albumin, fibrinogen etc.) which subsequently influences the adhesion of leukocytes, macrophages or platelets and ultimately leads to fibrous encapsulation. Thus, the adsorption of proteins could be one of the determinants of biocompatible nature of the material. The adsorption of BSA onto the prepared nanocomposites was performed by the batch process as reported elsewhere(24).

A known volume of protein solution of definite concentration is mildly shaken with the polymer composite matrix and the reaming concentration of protein was monitored in the solution spetrophotometrically. The amount of the adsorbed protein was calculated with the help of the following mass balance equation, (Eq. 3).

$$\text{Adsorbed amount(mg m}^{-2}) = \frac{(C_o - C_a)\text{V}}{\text{A}} \qquad (3)$$

Where, Co and Ca being the concentration of protein solution (mg per mL) before and after adsorption, respectively. V is the volume of the protein solution and A is the surface area of the adsorbent.

2.3.6.2. *Clot formation test.* The antithrombogenic potential of the composite surface may be judged by the blood clot formation test as described elsewhere (25). In brief, the PP-polymer composites are equilibrated with saline water (0.9% w/v NaCl) for 72 h in a constant temperature bath. To these swollen composites was added 0.5 mL of acid citrate dextrose (ACD) blood followed by the addition of 0.03 mL of $CaCl_2$solution (4 M) to start the thrombus formation. The reaction was stopped by adding 4.0 mL of deionized water and the thrombus formed is separated by soaking in water for 10 min at room temperature and then fixed in 36% formaldehyde solution (2.0 mL) for another 10 min. The fixed clot is placed in water for 10 min and after drying its weight is recorded.

2.3.6.3. *% Hemolysis tests.* Hemolysis experiments were performed on the surfaces of the prepared composites as described elsewhere (26). In a typical experiment, a dry composite disc is equilibrated in normal saline water (0.9% NaCl solution) for 24 h at 37°C for 24 h and human ACD blood (0.25 mL) was added into the gels. After 20 min, 2.0 mL of saline water was added on the surface to stop hemolysis and the sample is incubated for 60 min at 37°C. Positive and negative controls were obtained by adding 0.025 mL of human ACD blood and saline solution, respectively to 2.0 mL of distilled water. Incubated samples were centrifuged for 45 min, the supernatant was taken and its absorbance was recorded on a spectrophotometer at 545 nm. The percent of hemolysis was calculated using

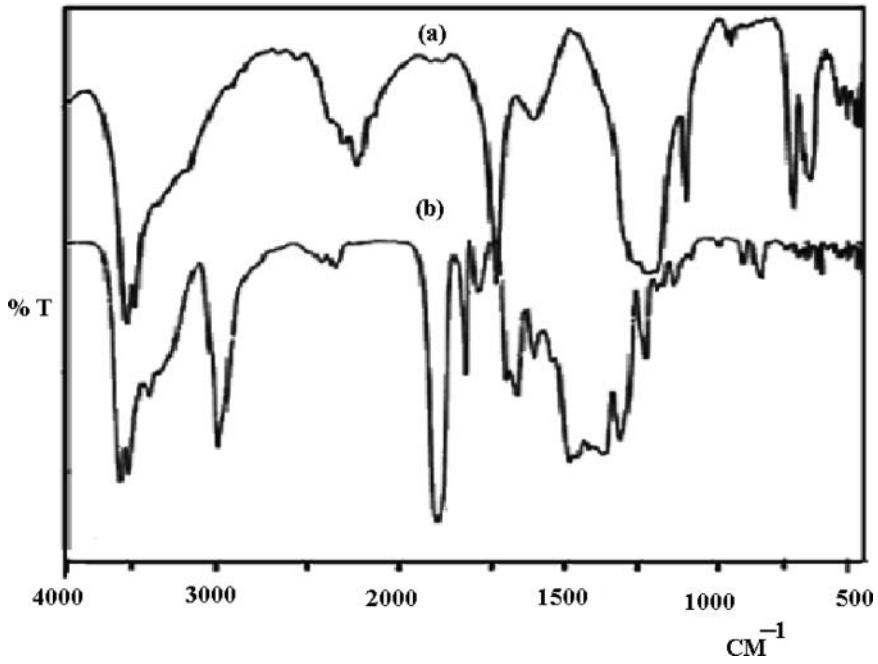

Fig. 3. FTIR spectra of (a) Pure plaster of Paris and (b) PP-HEMA composite.

the following relationship,

$$\% \text{ Haemolysis} = \frac{\text{A test sample} - \text{A } (-) \text{ sample}}{\text{A } (+) \text{ sample} - \text{A } (-) \text{ sample}} \quad (4)$$

Where A = Absorbance.

3 Results and Discussion

3.1 FTIR Studies

The FTIR spectra of pure plaster of paris and PP-HEMA composites are shown in Figure 3 (a) and (b), respectively. In Figure 3(a) strong bands in the region 1080 to1150 cm^{-1} and also medium to strong bands between 580 to 670 cm^{-1} clearly show the presence of the sulphate ions (SO_4^{2-}). The presence of hydroxyl bands in the area 3700 to 3100 cm^{-1} is convenient for distinguishing the different hydrates in the system $CaSO_4$-H_2O. The three types of $CaSO_4$: gypsum, hemihydrates and anhydrite, are easily identified just by the differences around 3500 cm^{-1} and by the different splitting of the peak around 1620 cm^{-1}(27).

The presence of HEMA in PP-HEMA composite is confirmed by the observed absorption bands at 1729 cm^{-1}.(C-O stretching), 1163 cm^{-1}.(O-C-C stretching), 3439 cm^{-1}. (O-H stretching), and 1469 cm^{-1}.(OH banding). The specta shows an asymmetric C-H stretch of a methylene group at 2946 cm^{-1}.

Broad band appears between 3000-3500 cm^{-1} in the spectra of the composite which clearly indicates the presence of intermolecular hydrogen bonded OH groups of PVA and PP-HEMA composite.

3.2 XRD Studies

The change in XRD pattern of the conversion of PP crystalline phase to the PP-HEMA composite was evaluated by conducting XRD analysis of PP and prepared composite as shown in Figures 4a and 4b, respectively. As shown in

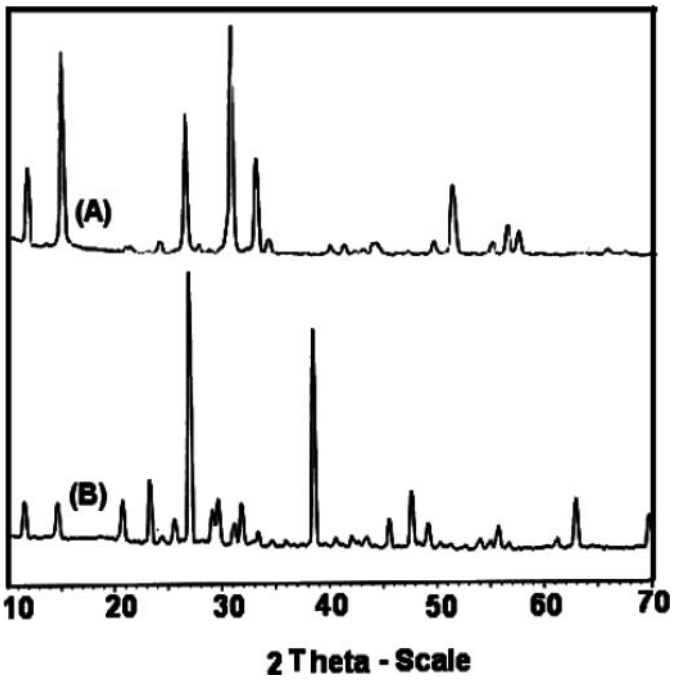

Fig. 4. XRD of (a) Pure plaster of paris and (b) PP-HEMA composite.

Figure 4(a) several characteristic sharp peaks at 2θ values of about 15°, 25°, 30° and 32°, respectively of varying intensities were deducted which clearly confirm the presence of well crystallized PP phase. Figure 4b shows the XRD for PP-HEMA composite with slight broadening of the apatite peaks showing the decrease in crystallinity of PP because of incorporation of organic polymer matrix. The prominent XRD peaks at about 27° and 38° of almost equal intensities show well crystalline nature of PP even in composite state. The spectra (b) also show a small peak at 20°, 2θ value, which is indicative of (100) plane of PVA. The mean grain size was calculated using Debye-Scherrer formula (28, 29) as shown in Equation 5,

$$d = \frac{k\lambda}{\beta \cos \theta} \quad (5)$$

Where d is mean grain size, k is the shape factor (0.9), β is broadening of the diffraction angle and λ is diffraction wavelength (1.54 Å). The estimated average grain size of PP was found to be 7.77 nm.

The physical and mechanical properties of the polymers are profoundly dependent on the degree of crystallinity. All the X-ray diffraction methods reported in literature for calculating the crystallinity in polymer are based on the following assumptions:

(1) The scattering capacity of crystallite is equal to that in amorphous with the same mass.
(2) The intensity of the X-rays scattered from the specimen is approximately equal to the sum of that from the crystalline and amorphous in the specimen .

The % crystallinity has been calculated for the irradiated PP-HEMA composites using the expression given in literature (30). The numerical formula to calculate % crystallinity (%X) has been given in the following Equation 6,

$$\%\text{Crystallinity} = \text{Ic} / \text{Ia} + \text{K.Ia} \quad (6)$$

Where Ic and Ia are the integrated intensities of crystalline and amorphous peaks respectively, K is a constant taken as unity (31). Areas of the peaks were determined by the "cut and weight method". The relation between integrated intensities and area of crystalline and amorphous peaks has been evaluated from the literature (32). It has been found that the % crystallinity of the composite containing 1.64 mM HEMA and 4.0 g PP was calculated to be about 10.32.

3.3 SEM Studies

The morphology of a biomaterial contributes significantly to its biocompatibility and thus, realizing this important aspect the morphology of the surface has been examined by recording SEM images of the PP-HEMA composites. The SEM images of the composites are shown in Figure 5 which clearly show that the composite surface is highly porous in nature and PP crystals are present as aggregated clusters of cylindrical shape. The size of the aggregated crystals varies in the range 10 to 20 μm having an average width of 5 μm.

3.4 Mechanical Testing

The mechanical properties of the prepared nanocomposites were evaluated in terms of compressive strength and modulus, respectively. The results summarized in Table 1 clearly indicate that the compressive strength of nanocomposites varies in the range 4.5 to 16 MPa whereas the modulus varies in the range 33 to 200 MPa. The data are in good agreement with those of the trabecular bone which is reported to have compressive strength and Young's modulus ranging between 2–10 MPa and 50–100 MPa, respectively

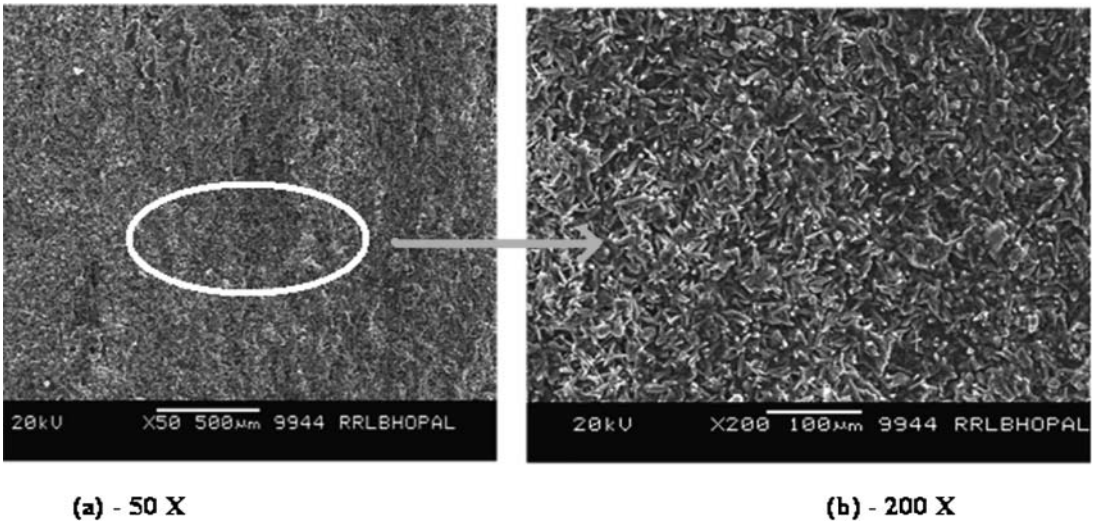

Fig. 5. The SEM images of PP-HEMA composite.

Table 1. Data showing the compressive strength and modulus of PP-HEMA composites of different compositions

Variation of content in composite	*Concentration*	*Compressive strength (in MPa)*	*Modulus (in MPa)*
PVA	0.5 g	4.5	33
PVA	2.0 g	5.2	50
HEMA	4.1 mM	10.2	100
HEMA	20.6 mM	12	200
EGDMA	0.53 mM	7.7	50
EGDMA	2.12 mM	6.4	100
PP	2.0 g	15	200
PP	5.0 g	16	100

(33). This clearly suggests that by a proper selection of the chemical composition of the nanocomposite the desired mechanical properties may be achieved.

3.5 Swelling Behavior of Composites

One of the prime factors to contribute to biocompatible nature of synthetic biomaterials is the amount of water content which imparts several unique physiochemical properties to the material. A polymer matrix imbibing an adequate of water, shows living tissue like membrane, physiological stability, low interfacial tension, permeability to biomolecules, etc. Thus realizing the unusual significance of water sorption capacity of a material, the PP-HEMA composites have been investigated for water sorption capacity and the influence of chemical composition of the composites on their water intake has been investigated as discussed below:

3.5.1. *Effect of PVA*

The influence of increasing amount of PVA on the degree of water sorption has been investigated by varying PVA in the range 0.5 g to 2.0 g in the feed mixture of the composite. The results depicted in Figure 6 indicate that the swelling ratio initially increases and then decreases with an increasing amount of PVA. The observed results may be explained by the fact that with the initial increase in PVA concentration the hydrophilicity of the composite increases, which results in an enhanced swelling ratio. However, beyond 1.0 g of PVA content, the volume fraction of polymer in the composite increases which enhances the degree of interaction between the PVA-PVA and PVA-HEMA molecules, thus increasing the extent of crosslinking in the hydrogel which eventually results in a fall in the swelling ratio.

When the results are analyzed in the light of the mechanisms of the composite formation, it appears quite convincing that with an increasing number of PVA molecules in the PVA-PP-HEMA composite in aqueous solution, a greater number of hydrogen bonds shall be established between PVA-PVA and PVA-HEMA molecules. In the same way with increasing richness of PVA in polymer mixture, the formation of PVA crystallites is favored, which also results in a lesser degree of swelling. Similarly, when PVA concentration becomes greater, the phase separation becomes more likely and this, consequently, lowers the swelling ratio.

3.5.2. *Effect of HEMA*

The swelling ratio of the composite is also influenced by the PHEMA content in the composite. It is clear from Figure 7 that when the concentration of monomer (HEMA) increases from 4.1 mM to16.4 mM in the feed composition, the swelling ratio increases, while beyond 16.4 mM of HEMA content of the gel, the swelling ratio decreases. The

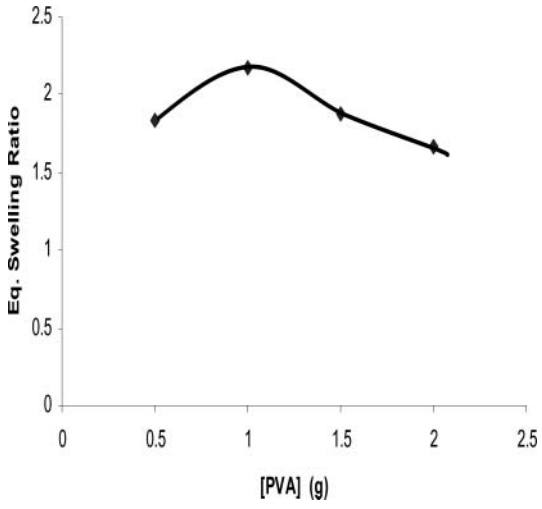

Fig. 6. Effect of PVA on swelling ratio.

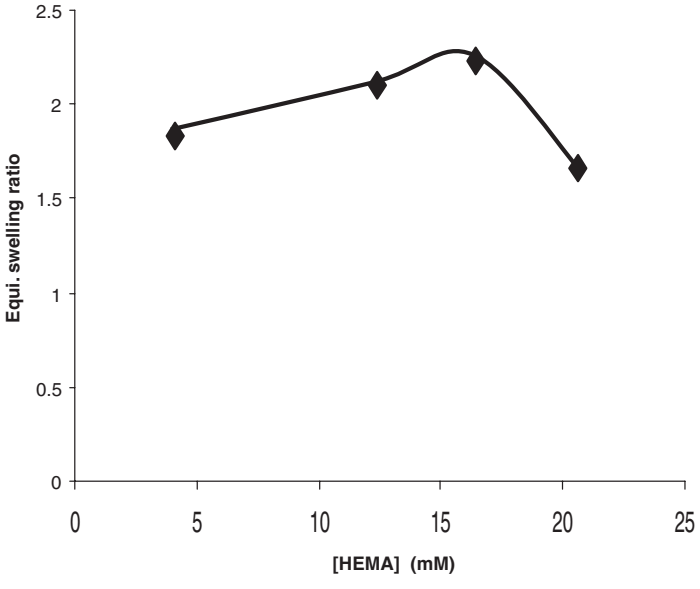

Fig. 7. Effect of HEMA on swelling ratio.

observed initial increase in swelling ratio may be attributed to the fact at higher monomer concentration, the molecular weight of PHEMA chains also increases, which results in longer chains, thus creating wider voids in the nanocomposite. Thus, a matrix with larger pores accommodate more water and, consequently, results in a greater water sorption.

At a much higher concentration (i.e. beyond 16.4 mM) of HEMA, the observed decrease in the swelling ratio may be attributed to the fact that with an increasing number of PHEMA molecules, the possibility of hydrogen bond formation between hydroxyl groups also increases which may result in interpenetration and entanglements of polymer chains. Consequently, the gel may become compact with reduced mesh sizes which will obviously bring about a fall in the water sorption.

3.5.3. *Effect of Plaster of Paris (PP)*

Upon impregnation, the bonding between particles of PP and polymer phase of HEMA brings about a significant change in water sorption behavior. In order to observe its effect, the amount of PP was varied in the range 2.0 g to 5.0 g in the feed mixture. The results shown in Figure 8 clearly reveal that the swelling ratio constantly increases with increasing PP content in the composite. The results are fully expected and may be explained by the fact that due to higher hydrophilicity of PP, its increasing amount in the composite results in a higher water sorption by the composite. Alternatively, the increasing polymer-PP interactions with increasing amount of PP lead to stabilize the polymer chains so that the swelling ratio increases.

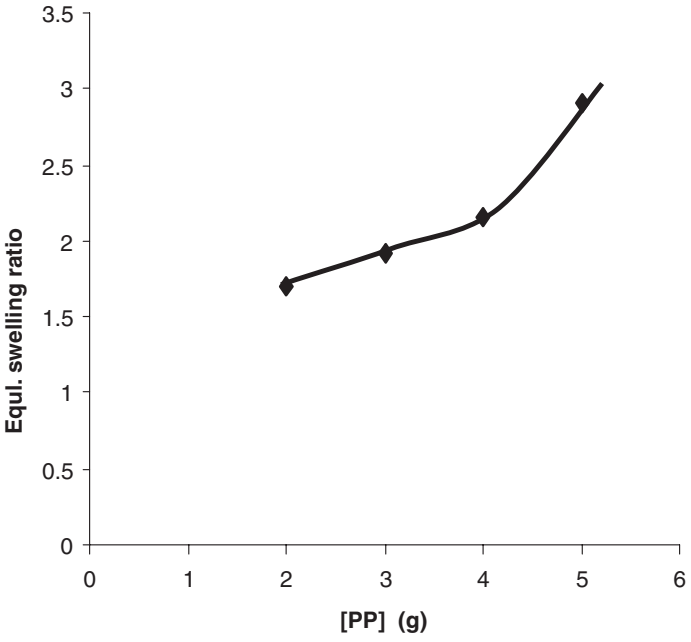

Fig. 8. Effect of PP on swelling ratio.

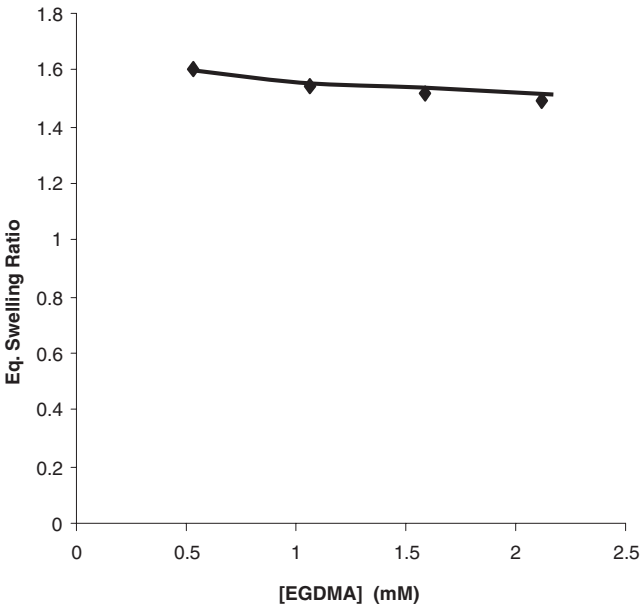

Fig. 9. Effect of EGDMA on swelling ratio.

3.5.4. *Effect of EGDMA*

The crosslinker has a pronounced effect on the swelling ratio of the composite. When the EGDMA concentration is raised in the feed mixture in the range 0.53 mM to 2.12 mM, the degree of water sorption decreases as shown in Figure 9. The decrease noticed in the composite may be contributed to the reason that a greater concentration of crosslinker produces a compact network with greater number of crosslink density The pore sizes of composite also decrease which may result in a lower degree of swelling. It has also been reported (34) that the introduction of a crosslinker often tends to raise the glass transition temperature (Tg), which consequently results in restrained mobility of polymer chains. This, in turn, lowers the water sorption capacity of the polymer composite.

3.5.5. *Effect of pH*

In the present investigation, the influence of pH on the swelling ratio of the composite has been studied by varying pH of the swelling medium in the range 4.0 to 11.0. The results are shown in Figure 10, which clearly reveal that the swelling ratio of composite increases up to pH 7 achieving an optimum swelling and thereafter decreases with further increase in pH (35). The results may be explained below.

The observed increase in swelling ratio with increasing pH of the swelling may be attributed to the fact that as the pH rises, some of the ester bonds of PHEMA chain may get hydrolyzed and procedure carboxylate bearing anionic chains which, due to repulsion forces, may relax the network chains, thus accommodating larger amounts of water.

However, beyond pH 7.0, the swelling ratio decreases, which may be due to the decreasing ionic osmotic pressure

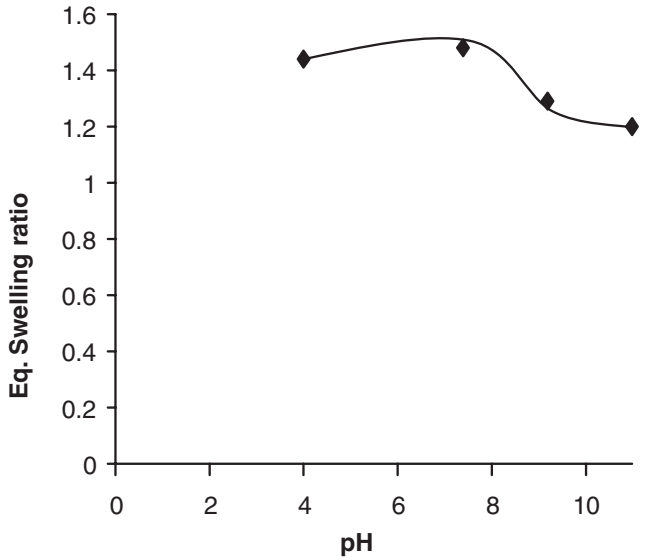

Fig. 10. Effect of pH on PP-HEMA composite.

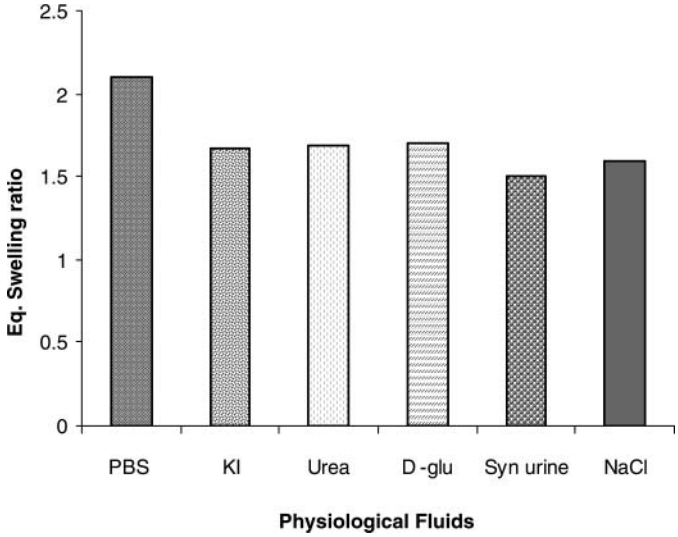

Fig. 12. Effect of biological fluids on PP-HEMA composite.

as predicted by the well known Donnan membrane theory (36).

3.5.6. *Effect of Temperature*

The influence of temperature on the swelling of composite is of great significance because it directly controls diffusion of water molecules into the matrix, segmental mobility of the network chains and water polymer interaction in the present study. The effect of temperature on equilibrium water sorption has been investigated by carrying out water sorption experiments in the range 10 to 45°C. The results are presented in Figure 11, which clearly indicates that the swelling ratio markedly increases up to 30°C temperature of the swelling medium, while thereafter a fall is observed.

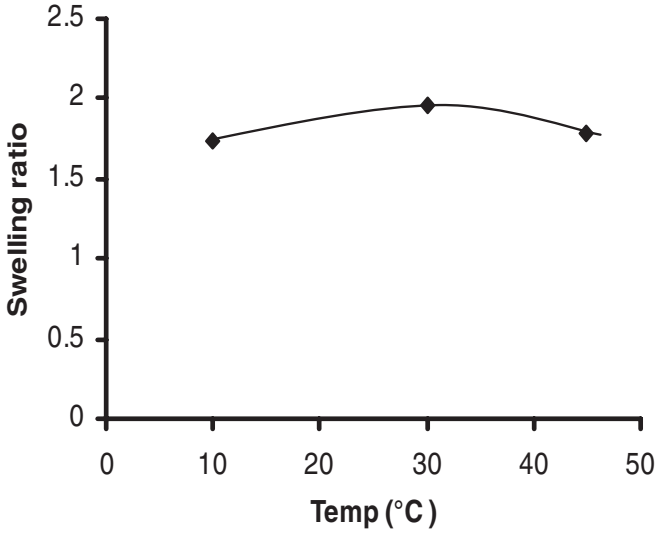

Fig. 11. Effect of temperature on PP-HEMA composite.

The results may be explained by the fact that when the temperature is increased, both the segmental mobility of the composite chains and diffusion of water molecules into the matrix increase which obviously results in greater swelling. However, beyond 30°C, a decrease in equilibrium swelling may be explained due to the breaking up of hydrogen bonds between water molecules and polymer chains.

3.6 Stability in Biofluids

In many biomedical applications, the implanted device often comes in contact with physiological biofluids for intended period of time in the body and, therefore, studying the impact of on biofluids on water sorption is worthwhile.

For assessing the stability of the composite, they were swollen in solutions such as KI (15% w/v), urea, D glucose (5% w/v) and in physiological fluids like saline water (0.9%NaCl) and synthetic urine. Swollen weights were recorded at a definite time period and results are shown in Figure 12. It is clear from the data that the swollen composites do not lose any weight with time which, clearly suggests fair stability in biological fluids. This obviously rules out any possibility of erosion, disintegration or chemical degradation of the matrix.

3.7 Percent Porosity

Porosity characterization is based on the presence of open pores, which are intimately related to the chemical composition of the nanocomposite. Thus, the influence of chemical composition on the percent porosity of the matrix properties such as permeability, and surface area of the porous structure. The measured porosity of the PP-HEMA composites is summarized in Table 2. The results have been investigated by varying concentration of the components

Table 2. Data showing the percent porosity of PP-HEMA composites of different compositions

PVA (in g)	*PP (in g)*	*HEMA (inMm)*	*EGDMA (inMm)*	*% Porosity*
0.5	4.0	16.4	1.06	39
1.0	4.0	16.4	1.06	42
1.5	4.0	16.4	1.06	47
2.5	4.0	16.4	1.06	49
1.0	2.0	16.4	1.06	34
1.0	3.0	16.4	1.06	31
1.0	4.0	16.4	1.06	30
1.0	5.0	16.4	1.06	29
1.0	4.0	4.10	1.06	41
1.0	4.0	12.3	1.06	39
1.0	4.0	16.4	1.06	30
1.0	4.0	20.6	1.06	28
1.0	4.0	16.4	0.53	37
1.0	4.0	16.4	1.06	42
1.0	4.0	16.4	1.59	43
1.0	4.0	16.4	2.12	52

of the matrix the results summarized in Table 2 may be discussed as below.

When the amount of PVA increases from 0.5 g to 2.5 g, the % porosity increases from 39 to 49 and may be explained by the fact that increasing amount of PVA results in a large number of PVA chains which upon being grafted by HEMA chains give rise to three dimensional structures with enhanced internal voids. This obviously results in increased porosity. The inorganic component of the composite is PP and when its increasing amounts are added into the percent, porosity is reduced from 34 to 29. The observed decrease is attributed to the fact that the added PP fills up the internal voids of the composites, thus reducing the extent of porosity. A similar decrease in percent porosity is noticed from 41 to 28 when the concentration of HEMA increases from 4.10 to 20.6 mM. The observed decrease in porosity may be explained on the basis of polymerization chemistry. As the concentration of HEMA increases, the long chains of HEMA are produced due to increase in molecular weight of PHEMA macromolecules. These longer chains form wider pores and, therefore, percent porosity decreases.

In the case of crosslinker (EGDMA) variation, the percent porosity increases from 37 to 52 with increasing crosslinker concentration in the range 0.53 to 2.12 mM. The observed increase in porosity is quite obvious as the nanocomposite with a larger number of crosslink forms greater number of voids and, therefore, leads to enhanced porosity.

3.8 Blood Compatibility

Blood compatibility of a material is intimately related to various intrinsic factors such as organization of water molecules in the polymer matrix, chemical architecture and topology of the surface etc. In the present study, also various *in vitro* tests were applied to observe the blood compatibility of the prepared PP-HEMA composite. The results are shown in Table 3, which may be discussed as below.

The results reveal that the weight of blood clot constantly decreases with increasing the amount of HEMA and PVA in the feed mixture. The results may be explained on the basis of the fact that both HEMA and PVA are hydrophilic polymers and therefore, are not expected to provoke any damage to blood cells or any change in the structure of the plasma proteins. It has also been realized that with increasing concentrations of HEMA and PVA, the composite acquires more smoothness of their surfaces and this consequently results in an improvement in antithrombogenic

Table 3. Data showing blood compatibility parameters of PP-HEMA composites of varying compositions

PVA (in g)	*PP (in g)*	*HEMA (in Mm)*	*EGDMA (in Mm)*	*BSA adsorption [mg g^{-1}]*	*Percentage haemolysis*	*Blood clot formation [mg]*
0.5	4.0	16.4	1.06	0.032	20.6	29.0
1.0	4.0	16.4	1.06	0.029	19.3	27.0
1.5	4.0	16.4	1.06	0.025	19.0	23
2.5	4.0	16.4	1.06	0.024	16.2	20
1.0	2.0	16.4	1.06	0.022	15.4	9
1.0	3.0	16.4	1.06	0.026	18.5	12
1.0	4.0	16.4	1.06	0.030	22.2	18
1.0	5.0	16.4	1.06	0.033	23.0	21
1.0	4.0	4.10	1.06	0.029	18.3	33
1.0	4.0	12.3	1.06	0.024	15.2	27
1.0	4.0	16.4	1.06	0.021	13.7	24
1.0	4.0	20.6	1.06	0.020	13.2	23
1.0	4.0	16.4	0.53	0.025	10.3	23
1.0	4.0	16.4	1.06	0.027	12.6	27
1.0	4.0	16.4	1.59	0.030	17.9	30
1.0	4.0	16.4	2.12	0.031	8.2	33

property of material. The prepared composites were tested for haemolytic activity and the results obtained are quite satisfactory. Percent haemolysis is maximum (100%) for a distilled water added blood sample (positive control). The results obtained clearly indicate that, with increasing HEMA and PVA content, the extent of haemolysis steadily decreases. The observed results may be attributed to the reason that, with the increase in HEMA and PVA weight fractions in the composite, the surface composition favorably changes, which improves the blood compatible quality of the material.

One of the essential components of the composite is PP and its concentration in the composite is expected to influence blood compatibility of the matrix. In order to examine this, concentration of PP powder was varied in the range 2.0 to 5.0 g and blood compatibility parameters were evaluated. The data summarized in Table 1 reveal that with increasing PP content, the blood compatibility of the composite shows a decrease, i.e. all the three parameters increase. The reason for the observed increased thrombogenicity is that the ionic groups of PP may react with the blood components and produce greater blood-surface interactions. This is likely to cause thrombogenic behavior of the composite.

When the concentration of crosslinker is raised in the range 0.53 to 2.12 mM, the amount of blood clot formed increases with increasing EGDMA content in the composite. The results also reveal that both the percent haemolysis and protein adsorption increase with increasing EGDMA content. The results obtained are consistent with each other and suggest that the composite shows decreasing blood compatibility with increasing number of crosslink. The results may be explained by the fact that since EGDMA is a hydrophobic crosslinker, its increasing content results in greater protein-surface interaction and, therefore, shows more clot formation and percent haemolysis.

The above discussion clearly suggests that a less crosslinked composite with more PVA and low PP content may prove to be more biocompatible.

4 Conclusions

Polymerization of 2-hydroxyethyl methacrylate (HEMA) in the immediate presence of polyvinyl alcohol (PVA) and plaster of paris (PP) results in a nanocomposite type of material which shows a fair level of resemblance to natural bone and opens up a synthetic route to design bone type of materials with simple polymerization chemistry.

The FTIR spectral characterization of the material clearly indicates the presence of PVA, PHEMA and PP in the nanocomposite material. Whereas the SEM of the composite material suggests porous morphology, the size of the aggregated crystals of the PP was found to vary in the range 10 to 20 μm. The XRD spectra reveal a semi-crystalline nature of the composite matrix and the size of the nanocrystal of the PP was estimated to be nearly 8 nm as calculated from the Debye-Scherrer equation.

The compressive strength of nanocomposites varies in the range 4.5 to 16 MPa, whereas the modulus varies in the range 33 to 200 MPa which are quite comparable to the corresponding values of the trabecular bone.

The composites show adequate water sorption capacity, which varies with the chemical composition of the material. When the amounts of PVA and HEMA were varied in the studied range, the swelling ratio initially increases and then decreases. On the other hand, a constant in water uptake capacity was noticed with increasing PP and EGDMA (crosslinker) content in the composite. The optimum swelling capacity is exhibited by the nanocomposite at neutral pH and normal temperature (30°C).

The porosity of the matrix increases significantly with increasing content of PVA whereas a fall in porosity is noticed with increasing concentration of crosslinker PHEMA, PP, and crosslinking agent (EGDMA). The composites were quite stable in various simulated biological fluids.

The blood compatibility results reveal that the weight of blood clot constantly decreases with increasing amount of HEMA and PVA in the feed mixture. It has also been realized that with increasing concentrations of HEMA and PVA, the composite acquires more smoothness of their surfaces and this consequently results in an improvement in antithrombogenic property of the material. The in vitro blood compatibility results also indicate that with increasing HEMA and PVA content, the extent of haemolysis steadily decreases. The nanocomposites show a reduced blood compatibility with increased crosslinker content. Thus, by a proper manipulation of the composition of the matrix, a desired material with elevated blood compatibility may be achieved.

Acknowledgments

The authors wish to acknowledge the authorities of Regional Research Laboratory, Bhopal (MP), India for carrying out SEM, Compressive strength and XRD analysis of the nanocomposite samples.

References

1. Boonen, S. (2004) *J. Intern. Med.*, 255:1–12.
2. Tamenoff, J.S. and Mikos, A.G. (2005) *Biomate.,* 21, 2405–2412.
3. Boulpaep, Emile, L. and Boron, Walter, F.: Medical physiology; a cellular and molecular approach, Philadelphia, Saunders ISBN 1416023283, 1089–1091, 2005.
4. Hall, M.J., Owings, M.F.: Hospitalizations for injury, 2000 National Hospital Discharge survey, Hyattsville Maryland.U.S. National Center for Health Statistics, United States, 329, 1–18, 2002.
5. Ramakrishna, S., Jayer, J., Wintromantel, E. and Leong, K.W. (2001) *Comp. Sci. Technol.*, 61, 1189–1224.
6. Dietmar, W. Hutmacher (2000) *Biomaterials*, 21, 2529–43.

7. Buchoz, R.W. (2002) *Clinical Orthopd.*, 395, 44–52.
8. Goel, SC. (2003) *Ind. J. of Orthopd.*, 37:143–144.
9. Frame, J.W. (1975) *J. Dent.*, 3, 177–187.
10. Kanellakopolou, K. and Giamarellos–Bour boulis, Ej. (2000) *Drugs*, 59, 1223–1232.
11. Bajpai, A.K. and Mishra, D.D. (2004) *J. Mater. Sci.: Mater. Med.*, 15, 83–592.
12. Song, J., Malathong, V. and Bertozzi, C.R. (2005). *J. Am. Chem. Soc.*, 127, 3366–3372.
13. Mendes, S.C., Reis R.L., Bovell Y.P., Cunha A.M., van Blitterswijk, C.A., de Bruijn, J.D. (2001) *Biomaterials,* 22, 2057–2064(8)
14. Xu, X. and Huang, J. (2004) *J. Polym. Sci. Part A Polym. Chem.*, 42, 5523–5529.
15. Heness, G. and Ben-Nissan, B. *Mater. Forum,* 27, 104–114 (2004).
16. Ma, P.X., Zhang, R.Y., Xiao, G.Z. and Franccschi, R.J. (2001) *J. Biomed. Mater. Res.,* 54, 284–293.
17. Brigger, I., Durbernet, C. and Couvreur, P. (2002) *Adv. Drug Deliv. Rev.,* 54, 631–651.
18. Chouhan, R. and Bajpai, A.K. (2009) *J. Mater. Sci.: Mater. Med.,* 20, 1103–14.
19. Wang, Jwo-lin, Zin,Ying-Tai, Tzeng, Ching-Cherng, Lin, Chin-I, Lin, Shi-Wei, Chang, Guan-Liang, (2003) *J. Med. Bio. Eng.,* 23, 205–212.
20. Lou, X., Chirila, T.V. and Clayton, A.B. (1997) *Int. J. Polym. Mater.,* 37, 1–14.
21. Bajpai, A.K. and Saini, R. (2006) *J. Mater. Sci.: Mater. Med.,* 17, 49–61.
22. Sepulveda, P., Ortega, F.S., Innocentini, M.D. and Pandolfelli, V.C. (2000) *J. Am. Ceram. Soc.*, 83, 3021–3024.
23. Zhang, Y. and Zhang, M. (2001) *J. Biomed. Mater. Res,* 55, 304–312.
24. Bajpai, A.K. and Shrivastava, M., (2001) *J. Macromol. Sci.: Pure & Appl. Chem.,* 38, 1123–1139.
25. Bajpai, A.K. and Saini, R. (2005) *Polym. Int.,* 54, 796–806.
26. Bajpai, A.K. and Saini, R. (2005) *Polym. Int.,* 54, 1233–1242.
27. Zender, K. and Arnold, A. (1984) *Studies in Conservation*, 29, 32–34.
28. Rahaman, M.N.: Ceramics processing and sintering. Marcel Dekker: New York, 1995.
29. Prabakaran, K., Thamaraiselvi, T.V. and Rajeswari, S. (2006) *Trends Biomater. Artif. Org.*, 19, 84–87.
30. Hussain, R., Qadeer, R., Ahmed, M. and Saleem, M. (2000) *Turk. J. Chem.,* 24:177–184.
31. Johnson, J.E. (1959) *J. Appl. Polym. Sci.*, 2, 205–209.
32. Ning, Y. (1989) *J. Polym. Sci.*, 7, 315–321.
33. Magnussen, R.A., Guilak, F. and Vail, T.P. (2005) *J. Orthopd. Res.*, 23, 576–583.
34. Ramaraj, B. and Radhakrishnan, G. (1994) *Polym.*, 35, 2167–2173.
35. Hassan, C.M. and Pappas, N.A. (2000) *J. Appl. Polym. Sci.*, 76, 2075–2079.
36. Flory, P.J.: Principles of polymer chemistry. Cornell University Press, 1953.